Structural, vibrational and thermodynamic properties of Ag_nCu_{34-n} nanoparticles

2009 J. Phys.: Condens. Matter 21 084220

(http://iopscience.iop.org/0953-8984/21/8/084220)

J. Phys.: Condens. Matter **21** (2009) 084220 (14pp) doi:10.1088/0953-8984/21/8/084220

Structural, vibrational and thermodynamic properties of Ag_nCu_{34-n} nanoparticles

Handan Yildirim, Abdelkader Kara and Talat S Rahman

Department of Physics, University of Central Florida, Orlando, FL 32816, USA

Received 11 August 2008, in final form 12 October 2008
Published 30 January 2009
Online at stacks.iop.org/JPhysCM/21/084220

Abstract

We report results of a systematic study of structural, vibrational and thermodynamical properties of 34-atom bimetallic nanoparticles from the Ag_nCu_{34-n} family using model interaction potentials as derived from the embedded atom method and invoking the harmonic approximation of lattice dynamics. Systematic trends in the bond length and dynamical properties can be explained largely from arguments based on local coordination and elemental environment. Thus an increase in the number of silver atoms in a given neighborhood introduces a monotonic increase in bond length, while an increase of the copper content does the reverse. Moreover, for the bond lengths of the lowest-coordinated (six and eight) copper atoms with their nearest neighbors (Cu atoms), we find that the nanoparticles divide into two groups with the average bond length either close to (∼2.58 Å) or smaller than (∼2.48 Å) that in bulk copper, accompanied by characteristic features in their vibrational density of states. For the entire set of nanoparticles, we find vibrational modes above the bulk bands of copper/silver. We trace a blue shift in the high-frequency end of the spectrum that occurs as the number of copper atoms increases in the nanoparticles, leading to shrinkage of the bond lengths from those in the bulk. The vibrational densities of states at the low-frequency end of the spectrum scale linearly with frequency as for single-element nanoparticles, with a more pronounced effect for these nanoalloys. The Debye temperature is found to be about one-third of that of the bulk for pure copper and silver nanoparticles, with a non-linear increase as copper atoms increase in the nanoalloy.

(Some figures in this article are in colour only in the electronic version)

1. Introduction

It has been widely accepted that a solid's surface representing the interface with the surrounding environment introduces differences in properties from those of the bulk form. These differences have opened new avenues through which one can fine-tune the physical and chemical properties and so approach the goal of designing materials with tailored characteristics. Because of their large surface-to-volume ratio, nanoparticles are good candidates for materials with novel and controllable properties. Efforts have thus been made to understand the size-dependent evolution of the physical, chemical, and electronic properties of these nanoparticles [1]. These studies also point to the possibility of using nanoparticles as building blocks for cluster-assembled materials [2] with tailored properties and possible applications [3] in the biomedical, catalytic, optical, and electronic industries [4]. Since alloying offers a natural avenue for further controlling and modifying properties of nanoparticles, attention has been directed to synthesis, characterization, and observation of novel properties of bimetallic nanoparticles [5]. The latter have also found themselves to be the arena for testing theoretical developments in techniques that aim at sketching multidimensional potential energy surfaces to search for the equilibrium structures of atoms and molecules in complex environments. The competing roles of elemental specificity, relative strengths of bonds and cohesive energy, local coordination, and electronic and geometric structure interplay to provide materials whose stability is not always transparent or easily controllable. Hence, developing an understanding of the microscopic factors that relate structure to functionality is at the basis of the increasingly important field of computational material design,

and nanoalloys provide a bottom-up approach to tailoring the properties of materials through a systematic understanding of the relative importance of the diverse factors that constitute a local environment. The issues at the theoretical level extend from the description of the geometric structure of the nanoalloy, to establishment of stability criteria, to extraction of the relative effects of structural, electronic, and vibrational contributions in controlling alloy novel properties. In the case of bimetallic nanoparticles, symmetry and elemental size are also expected to play a role in influencing the geometric structure.

Recently, Rossi *et al* [4] have applied global optimization techniques to several bimetallic clusters of transition metal elements consisting of 30–40 atoms, using semi-empirical inter-atomic potentials [6]. They found very stable 'magic' clusters, characterized as core–shell polyicosahedra with high (calculated) melting points. Earlier molecular dynamics simulations [7] dealing with the growth of core–shell structures of larger clusters (a few hundred atoms) showed that Ni and Cu impurity atoms prefer subsurface locations inside Ag clusters and induce higher stability and melting temperatures. For six binary systems (Ag–Ni, Ag–Cu, Au–Cu, Ag–Pd, Ag–Au, and Pd–Pt), Rapallo *et al* [8] also examined the effects of size mismatch, alloying tendency (as compared to that in the bulk phase of Ag–Ni and Ag–Cu), and the tendency for surface segregation. Among these binary systems, Ag–Cu has the largest size mismatch. These pioneering studies have been very helpful in developing the framework for a systematic methodology for determining the geometric structure and stability criteria for nanoalloys [9]. The stage is now set for complementary studies; in particular, the effect of alloying on the vibrational characteristics of the nanoparticles remains to be explored. Such an examination is needed because of its relevance in determining relative structural stability in bulk [10] and surface alloys [11].

In this work we have thus undertaken a systematic examination of the effect of changing elemental composition on the local structure (bond lengths), vibrational dynamics, and thermodynamics for the case of 34-atom Ag–Cu nanoparticles (the Ag_nCu_{34-n} family). As a starting point we take the geometric structure of each nanoparticle to be that obtained by Rossi *et al* [4], while recognizing that *a priori* inclusion of vibrational entropy in initial searches for equilibrium configurations could have produced a different outcome. For the rest of the paper, we proceed as follows. In section 2 we discuss the theoretical details, while in section 3 we summarize our results into four sub-sections:

(1) section 3.1 describes the results of our analysis of the bond lengths;
(2) section 3.2 presents the alloying effect on the vibrational densities of states of these nanoparticles and local vibrational densities of states;
(3) section 3.3 summarizes the results of the analysis of the vibrational free energies;
(4) sections 3.4 discusses the mean square vibrational amplitudes of the atoms in these nanoparticles and the Debye temperatures of the nanoparticles;

finally, in section 4, we present our comprehensive conclusions.

2. Theoretical details

The starting configurations of the 35 nanoparticles of the family of Ag_nCu_{34-n} were established by Rapallo *et al* [8], who used a genetic algorithm scheme to find the minimum energy configuration using an empirical potential [6]. They showed that this family consists of 'magic' nanoparticles, which are characterized by the common property of a perfect core–shell structure with Ag atoms on the surface and Cu atoms inside the shell. In figures 1(a)–(f), we present the geometric structures of six representative nanoparticles showing the differences in the stoichiometry despite similarity in the core shell. In this study, the starting configuration of a given nanoparticle has been subjected to a further relaxation using the conjugate gradient method [12] with interaction potentials derived from the embedded atom method (EAM) [13]. In the case of copper and silver and their alloys, these potentials have proven to provide accurate structural as well as vibrational properties for bulk and surface systems [14]. We calculate the force constant matrix of the nanoparticles (in their equilibrium configuration) from the partial second derivatives of the interaction potential. The force constant matrix is necessary to determine the vibrational dynamics and hence the thermodynamical functions of these nanoparticles. The vibrational densities of states may be determined from the force constant matrix (D) of the nanoparticles by constructing the corresponding Green's function. From the trace of the Green's function matrix, the normalized vibrational density of states $\rho(\omega)$ is obtained:

$$G(\omega^2 + \mathrm{i}\varepsilon) = (I(\omega^2 + \mathrm{i}\varepsilon) - D)^{-1} \tag{1}$$

$$\rho(\omega^2) = -\frac{1}{\pi} \lim_{\varepsilon \to 0} \mathrm{Im}\,\mathrm{Tr}[G(\omega^2 + \mathrm{i}\varepsilon)] \tag{2}$$

$$\rho(\omega) = 2\omega\rho(\omega^2). \tag{3}$$

The local density of states ($\rho_i(\omega)$) of each atom in the nanoparticle is such that $\sum_{i=1}^{n} \rho_i(\omega) = \rho(\omega)$, where n is the number of atoms in the nanoparticles and can be determined from the diagonal elements of the imaginary part of the Green's function matrix. Once the vibrational densities of states are calculated, we can easily determine the thermodynamical functions in the harmonic approximation of lattice dynamics. The local vibrational free energies of each atom i and their mean square vibrational amplitudes and Debye temperatures are thus calculated using the equations below:

$$F_i^{\mathrm{vib}} = k_{\mathrm{B}}T \int_0^\infty \ln\left(2\sinh\left(\frac{\hbar\omega}{2k_{\mathrm{B}}T}\right)\right)\rho_i(\omega)\,\mathrm{d}\omega \tag{4}$$

$$\langle u_i^2 \rangle = \frac{\hbar}{2M} \int_0^\infty \frac{1}{\omega} \coth(\hbar\omega 2k_{\mathrm{B}}T)\rho_i(\omega)\,\mathrm{d}\omega \tag{5}$$

$$\theta_i^2 = \frac{3\hbar^2 T}{M k_{\mathrm{B}} \langle u_i^2 \rangle}. \tag{6}$$

In consideration of vibrational contributions to the relative stability of the system, the quantity of interest is the excess vibrational free energy which is defined as the excess over

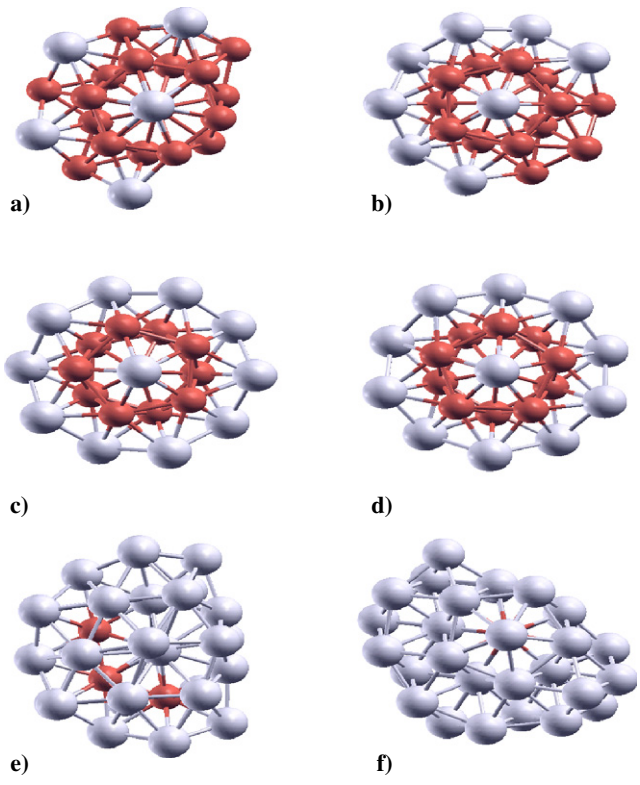

Figure 1. Structure of selected nanoparticles (**a**) Ag_9Cu_{25}, (**b**) $Ag_{12}Cu_{22}$, (**c**) $Ag_{16}Cu_{18}$, (**d**) $Ag_{17}Cu_{17}$, (**e**) $Ag_{31}Cu_3$ and (**f**) $Ag_{33}Cu_1$.

the values associated with the bulk system. Thus the local contribution to the vibrational excess free energy is given by

$$\Delta F_i^{\text{vib}} = F_i^{\text{vib}} - F_{\text{bulk}}^{\text{vib}} \tag{7}$$

where $F_{\text{bulk}}^{\text{vib}}$ is the bulk value (per atom) for the species (copper or silver) and is obtained from earlier calculations [15]. The total excess free energy (over the bulk), of course, contains a major contribution from the structural or potential energy and from configurational entropy. The excess potential energy portion is introduced by Ferrando *et al* [6] through the term Δ as expressed below in equations (8). We have similarly added a term which corresponds to the vibrational component of the excess energy (Δ_{vib}).

$$\Delta_{\text{pot}} = \frac{E_{\text{tot}}^{N,N_1} - N_1\varepsilon_1^{\text{coh}} - N_2\varepsilon_2^{\text{coh}}}{N^{2/3}} \qquad \text{and} \qquad \Delta_{\text{vib}} = \frac{F_{\text{tot}}^{\text{vib}} - N_1 F_{\text{bulk,Ag}}^{\text{vib}} - N_2 F_{\text{bulk,Cu}}^{\text{vib}}}{N^{2/3}} \tag{8}$$

where E_{tot}^{N,N_1} is the minimum energy for a given composition of the nanoparticles, $\varepsilon_1^{\text{coh}}$ and $\varepsilon_2^{\text{coh}}$ are the cohesive energies of the species (copper or silver), N_1 and N_2 are the numbers of Ag and Cu atoms, and N is the total number of atoms in the nanoparticle. The division by $N^{2/3}$ (approximately the number of surface atoms) yields the excess energy per surface atom. Here $F_{\text{tot}}^{\text{vib}}$ is the total vibrational free energy of the nanoparticle:

$$F_{\text{tot}}^{\text{vib}} = \sum_{i=1}^{N_1} F_{i,\text{Ag}}^{\text{vib}} + \sum_{i=1}^{N_2} F_{i,\text{Cu}}^{\text{vib}}. \tag{9}$$

$F_{\text{bulk,Ag}}^{\text{vib}}$ and $F_{\text{bulk,Cu}}^{\text{vib}}$ are the vibrational free energies of the bulk Ag and Cu atoms, respectively. The total excess energy is now written as

$$\Delta_{\text{tot}} = \Delta_{\text{pot}} + \Delta_{\text{vib}}. \tag{10}$$

In the above we have not included explicitly the contributions from configurational entropy, which come into play when deciding the relative stability of isomers corresponding to specific nanoalloy compositions. Such contributions were included by Rapallo *et al* [8] in their energetic considerations. Our interest here is a specific isomer.

3. Results and discussion

With the aim of investigating the combined effect of alloying and of the local elemental environment and coordination in determining the structural, vibrational and thermodynamical properties of this particular set of core–shell nanoparticles, we first provide a global analysis of the bond lengths between atoms in these 35 nanoparticles. We then calculate the total vibrational densities of states of the nanoparticles along with local vibrational densities of states of chosen atoms from this set of nanoalloys. Finally, we analyze such global and local thermodynamical quantities as free energy, mean square vibrational amplitudes and Debye temperatures.

3.1. Bond-length distribution in Ag_nCu_{34-n} nanoalloys

Since it is neither feasible nor desirable to present results of the bonding for all atoms in each of the 35 nanoparticles that form the Ag_nCu_{34-n} family, we choose to focus on those with the most dominant coordination. In contrast to the case of extended systems, the bond-length distribution is very broad; a criterion for counting neighbors is necessary. We have set the cut-off in the nearest-neighbor bond-length count at 2.7 Å and 3.1 Å, for copper and silver atoms, respectively. With these cut-offs in mind, we first tabulate the coordination of all atoms in each nanoparticle. The total number of Ag and Cu atoms, in the set of 35 nanoparticles, with specific coordinations, is divided by the total number of copper/silver atoms in the set (34×35) to obtain the number density. From the plots, in figures 2 and 3, of the number density as a function of coordination, we find that copper atoms with coordination 6, 8, 9 and 12 (with respective number densities of 0.2, 0.15, 0.27 and 0.29) and silver atoms with coordination 6, 8 and 9 (number densities of 0.51, 0.23 and 0.12, respectively) are the dominant ones. The number densities reflect the fact that these nanoalloys are of core–shell type, with copper atoms populating the core and silver favoring the shell. Moreover, one notes that in these small nanoparticles only 3% (7%) of the copper (silver) atoms form steps (coordination seven) and that corner/kink atoms with coordination six have a large density and even dominate: 51% in the case of silver. As for facets, one notes that for the case of copper atoms it is the dense (111) geometry that is favored, with 27% of the atoms (coordination nine), versus only 15% for the (100) geometry (atoms with coordination eight). The reverse is true for silver atoms, which show a preference for the more open structures, with 23% of the atoms on a (100) facet versus only 12% on the (111).

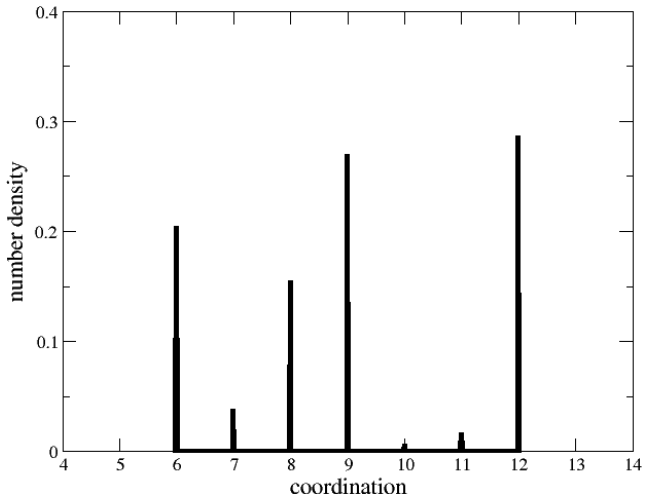

Figure 2. Number density for copper atoms as a function of coordination.

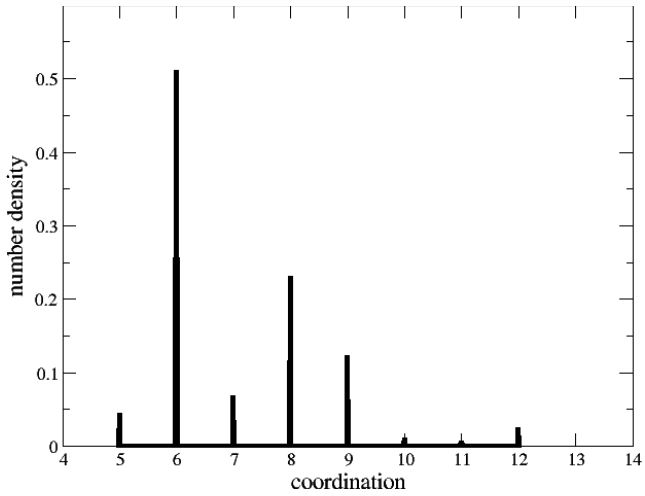

Figure 3. Number density for silver atoms as a function of coordination.

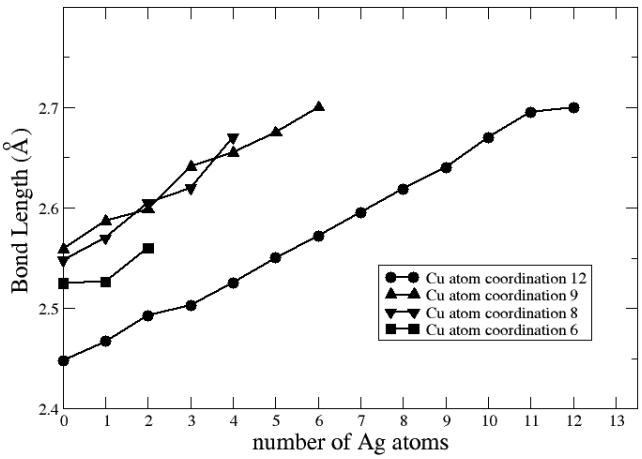

Figure 4. Variation of average nearest-neighbor bond length of Cu atoms with coordination and elemental environment.

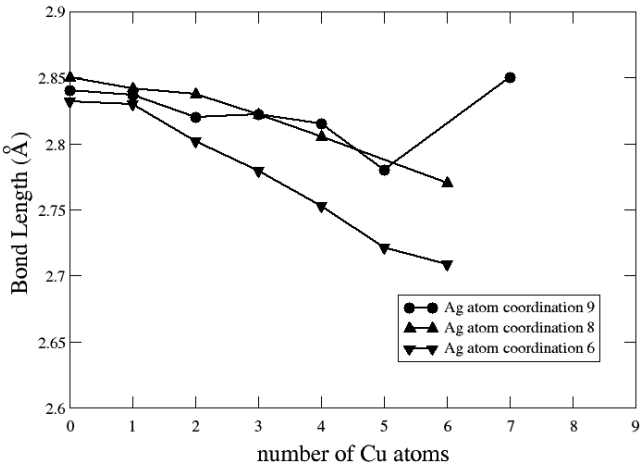

Figure 5. Variation of average nearest-neighbor bond length of Ag atoms with coordination and elemental environment.

As expected, there is a range of values for the average nearest-neighbor bond length for the silver (copper) atoms with the coordination of 6, 8 and 9 (12, 9, 8 and 6), which are discussed in the next paragraph. These changes in the average bond lengths for each coordination (changing the number of atoms of either species in the bonding) are shown in figures 4 and 5 for copper and silver, respectively. From figure 4, especially for coordination 12, we find a monotonic increase in the bond length as the number of silver atoms increases in the neighborhood. We find a similar behavior for the copper atoms with coordination 9 and 8, while for coordination 6 the statistics are too sparse to draw any specific conclusion.

For copper atoms with coordination 12 and no silver atoms in the neighboring sites, we find the average nearest-neighbor bond length to lie between 2.43 and 2.47 Å, with the exception of the Cu_{34} nanoparticle, for which the average bond length is 2.50 Å. With the addition of more Ag atoms to the neighborhood, the average nearest-neighbor distance increases monotonically from 2.43 Å (0 silver neighbors) to 2.70 Å (12 silver neighbors), an increase of about 0.02 Å per silver atom. This trend is obviously related to the fact that the bulk lattice constant of silver is larger than that of copper, and has consequences for the local thermodynamical properties, as we shall see. Note that the spread in the average bond length for any specific environment (for Cu atoms with fixed number of silver neighbors from any nanoparticle) is found to be small (of the order of 0.01–0.05 Å). For copper atoms with coordination nine, the average bond length also increases with the number of silver atoms in the neighboring sites: from 2.54 Å (no silver neighbors) to 2.71 Å (six silver neighbors), with variations in the average bond length between 0.02 and 0.07 Å. Similarly, for copper atoms with coordination eight the total increase in the average bond length is 0.14 Å as the number of neighboring silver atoms changes from 0 (2.53 Å) to 4 (2.67 Å), with a small variation within any given neighborhood (0.03–0.06 Å). Finally, for coordination six the same trend is found as for the case of other coordinations: an increase in the bond length on increasing the number of silver atoms. However, since the neighborhood shows a limited range of variation of the number of Ag atoms, the increase in the

Table 1. Average bond length for Cu atom with coordination six along with elemental environment (DFT calculations).

	Number of Ag atoms and bond length (Å)		
Cu coordination 6	0 Ag	1 Ag	2 Ag
$Ag_{18}Cu_{16}$	2.57(2.55)	—	—
$Ag_{16}Cu_{18}$	2.58(2.56)	—	—
$Ag_{15}Cu_{19}$	2.54(2.55)	—	—
$Ag_{14}Cu_{20}$	2.55(2.56)	—	—
$Ag_{13}Cu_{21}$	2.58(2.58)	—	—
$Ag_{12}Cu_{22}$	2.57(2.57)	—	—
$Ag_{11}Cu_{23}$	2.55(2.57)	2.58(2.60)	—
$Ag_{10}Cu_{24}$	2.52(2.51)	2.53(2.52)	2.56(2.56)
$Ag_{9}Cu_{25}$	2.57(2.58)	—	—
$Ag_{8}Cu_{26}$	2.51(2.51)	2.52(—)	—
$Ag_{7}Cu_{27}$	2.51(2.51)	2.53(2.54)	—
$Ag_{6}Cu_{28}$	2.48(2.47)	2.51(2.51)	—
$Ag_{5}Cu_{29}$	2.49(2.48)	2.52(2.51)	—
$Ag_{4}Cu_{30}$	2.49(2.48)	2.50(2.51)	—
$Ag_{3}Cu_{31}$	2.49(2.48)	2.50(2.50)	—
$Ag_{2}Cu_{32}$	2.49(2.49)	2.52(2.53)	—
$Ag_{1}Cu_{33}$	2.48(2.49)	2.55(—)	—
Cu_{34}	2.49(2.49)	—	—

average bond length is found to be not substantial. For copper atoms with coordination eight and six, an interesting trend in bond lengths is observed, particularly for those with no silver atom in the neighboring sites, for which the bond lengths divide into two groups. For the case of coordination eight, the first group of nanoparticles has the average bond length between 2.52 and 2.54 Å (smaller than bulk Cu), whereas for the second group the bond length varies from 2.56 to 2.59 Å (larger than bulk Cu). For atoms with coordination six, in the first group of nanoparticles the bond length lies between 2.48 and 2.51 Å. As the number of silver atoms in the nanoparticles increases from 9 to 18, the average bond length varies from 2.52 to 2.58 Å with a sudden shift for Ag_9Cu_{25}. This is also confirmed by our *ab initio* electronic structure calculations based on the density functional theory (DFT), which are summarized in table 1 in parenthesis. We should note that such behavior in the average bond lengths is not found for silver atoms. A more detailed analysis of our results will be presented elsewhere [16], and a DFT study on a particular nanoalloy ($Ag_{27}Cu_7$) is reported in [17].

As plotted in figure 5, the average bond lengths of silver atoms (with change in the number of copper atoms in the bonding) show that the effect of altering the elemental environment is in general much less pronounced than that for copper atoms. We find that there is almost a linear decrease in the bond length with the addition of copper atoms to the bonding. The case of silver atoms with coordination nine (seven copper neighbors) appears to violate the above trend (figure 5). However, for this coordination, the small number of such atoms in the family of nanoparticles does not produce sufficient statistics for drawing a definite conclusion. We also note that there is very little variation in the bond length for silver atoms with no copper atoms in the neighborhood. For the Ag atoms, the average bond length decreases with the addition of copper atoms to the environment from 2.84 Å (0 Cu) to 2.78 Å (5 Cu) for coordination nine, 2.84 Å (0 Cu) to 2.77 Å (6 Cu) for coordination eight and finally 2.83 Å (0 Cu) to 2.65 Å (6 Cu) for coordination six.

In summary, for the sets of copper (silver) atoms with coordination 12, 9, 8 and 6 (9, 8 and 6) we find the variation in the bond length to be 0.27, 0.17, 0.14 and 0.1 Å (0.07, 0.09 and 0.2 Å), respectively. We also find characteristic trends in bond-length variations induced by alloying, thereby providing the combination of coordination and local elemental environment as its (bond-length) measure.

We now proceed to examine whether the local coordination and the environment is an effective measure for determining other characteristics of the nanoalloys.

3.2. Vibrational densities of states of selected nanoalloys

When surface-to-volume ratio of a solid system becomes high as is the case with matter at the nanoscale, it is to be expected that a substantial contribution to the properties comes from the surface atoms. Earlier studies on nanoalloys by Ferrando and co-workers [18] showed that the melting temperature of these nanoparticles is relatively high compared to that of single-element nanoparticles of the same size. This may be a signature of hardening of the bond between atoms, which will have consequences for the vibrational densities of states (VDOSs) and hence for the thermodynamics of these nanoparticles. Hence, it is interesting to study the vibrational dynamics and thermodynamics of these systems and try to find any correlations to inter-atomic bonding. It will also be of interest to compare our findings with those already known for Ag and Cu surfaces, nanoparticles and bulk solid [15, 19–21].

In an earlier study of single-element (silver) nanoparticles of varying size (2–3.5 nm) [19], two features of the VDOS were found to be different from those of the bulk. One concerns the high-frequency end of the spectrum and the other the low-frequency portion. It was shown that the high-frequency end of the VDOS is shifted above that of the top of the bulk band, a fact that was traced to the shrinking of the nearest-neighbor distance of the specific atoms in the nanoparticles [19]. The shift in the high-frequency band was shown to be localized and to drop sharply with increasing size of the nanoparticles. At the low-frequency end, these nanoparticles exhibited substantial enhancement in the density of states as compared to that of the bulk spectrum. This enhancement was found to be the contribution of the outer atoms (surface atoms).

In the case of nanoalloys, not only the local coordination but also alloying is an important parameter affecting the VDOS. To illustrate the effect of alloying, we present in figures 6(a)–(f) the total VDOS of six selected nanoparticles ($Ag_{31}Cu_3$, $Ag_{27}Cu_7$, $Ag_{17}Cu_{17}$, $Ag_{10}Cu_{24}$, Ag_7Cu_{27} and Ag_3Cu_{31}) and compare the results to those of single-element nanoparticles Cu_{34} and Ag_{34}. We note a clear correlation at the high-frequency end of the spectrum with the change in the number of copper atoms in the nanoparticles. From figure 6(a), for the nanoparticle with only three copper atoms ($Ag_{31}Cu_3$), one can note a shift towards the high-frequency end of the spectrum as compared to the case of the pure 34-atom silver nanoparticle (Ag_{34}), as shown in the figure. This effect (alloying) becomes stronger for the other cases, which

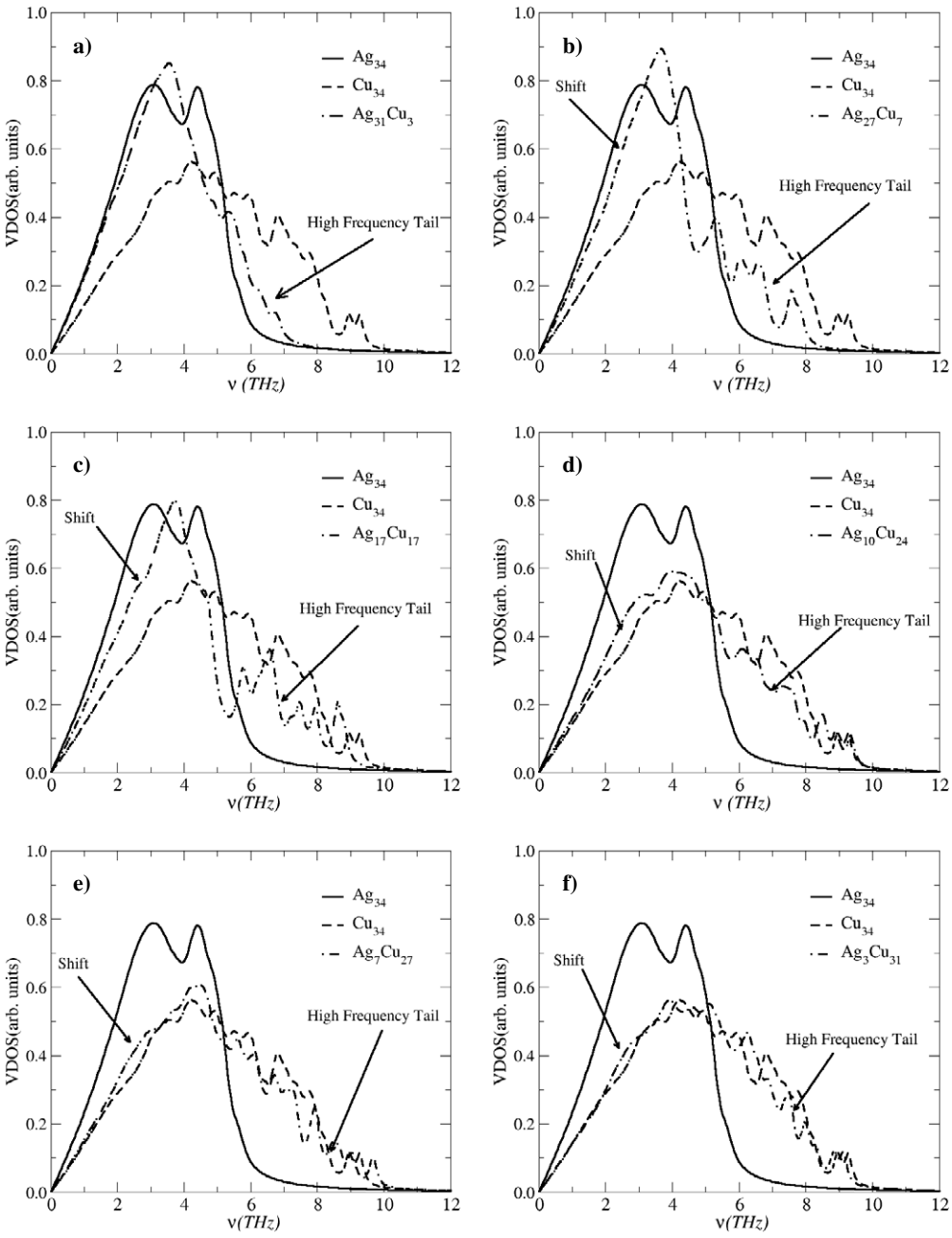

Figure 6. Vibrational densities of states (VDOS) of selected nanoparticles: (**a**) $Ag_{31}Cu_3$, (**b**) $Ag_{27}Cu_7$, (**c**) $Ag_{17}Cu_{17}$, (**d**) $Ag_{10}Cu_{24}$, (**e**) Ag_7Cu_{27} and (**f**) Ag_3Cu_{31}.

have increased alloying of Ag with Cu. One should also note that the shift towards the high-frequency end of the spectrum is found to extend over few terahertz (over the top of the bulk band). In figures 6(a)–(f), with increasing number of copper atoms, we note that the spectrum becomes close to that of the single-element Cu nanoparticle (Cu_{34}), as is to be expected. To quantify the effect of alloying in these nanoparticles, we have calculated the percentage (relative partial integral) of the VDOS in the high-frequency region above 5.1 THz (the frequency at which the VDOS of Ag_{34} is almost zero). In figure 7, we show this percentage as a function of the number of copper atoms in the system and find the dependence to be nearly linear. The small deviation from linear behavior in figure 7 is understandable given the simplicity with which the information has been extracted. The behavior at the low-frequency end of the spectrum for the chosen nanoalloys is found to be similar to that for single-element nanoparticles, for which the VDOS scales linearly with the frequency [19].

Below, we examine more closely the effect of environment on the dynamical properties of the nanoalloys by calculating the local vibrational densities of states (LVDOSs) for chosen copper (silver) atoms with coordination 12, 9, 8 and 6 (9, 8 and 6) respectively.

3.2.1. Local vibrational density of states of copper atoms in selected nanoparticles. Our analysis of the local

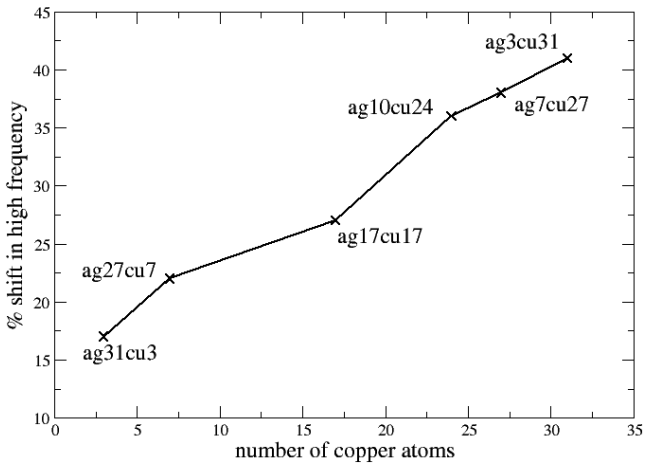

Figure 7. Percentage shift in the high-frequency end (above 5.1 THz) for selected nanoparticles.

vibrational dynamics relies on the analysis of bond length just presented. The vibrational dynamics of the copper atoms (with coordination 12, 9, 8 and 6 and varying environment) from the nanoparticles of selected composition along with the bulk densities of states of a copper atom are shown in figures 8(a)–(e). For the atoms with coordinations other than six, we have chosen arbitrarily one such atom from the family of the nanoparticles, since we find very little spread in the bond lengths. However, for coordination six we need to be careful, since the bond lengths (see table 1) fall into two categories, 'larger than bulk value' and 'smaller than bulk value', as discussed above. We examine the vibrational dynamics of these representative atoms from each of the two categories to ascertain any differences in the spectra.

From the LVDOS of copper atoms with coordination 12 (see figure 8(a)), the first observation is of the appearance of new peaks at 8.5 and 9.1 THz for environments containing zero and six silver neighbors (no peaks appear in these high-frequency range if there are 12 silver neighbors). The latter reflects softening in the Cu–Ag coupling introduced by the larger number of silver atoms. At the low-frequency end, we note an enhancement of the density of states, reflecting the induced softening of the bond by the presence of silver atoms. These features can be rationalized using bond-length arguments. We note that the bond length for copper atoms in these three environments is in the range of (2.41–2.53 Å) for zero, (2.50–2.74 Å) for six and finally (2.64–2.74 Å) for 12 silver neighbors. The shorter bond lengths are responsible for the high-frequency peaks at 8.5 and 9.1 THz (zero and six silver neighbors). For 12 silver neighbors, the shortest bond length (2.64 Å) is higher than the bond length in bulk copper (2.56 Å), thus explaining the absence of modes with frequencies above the Cu bulk band (see figure 8(a)). Larger bond lengths tend to indicate a softer bonding, which enhances the low-frequency end of the density of states. For example, for those copper atoms with 6 and 12 silver neighbors with large bond length (2.74 Å), there is an enhancement around 3 THz, which is absent for zero silver neighbors, whose maximum bond length is 2.53 Å. Similar arguments explain the features in the LVDOS of copper atoms with coordination nine with zero, three and six silver neighbors (see figure 8(b)).

Let us now turn to the case of copper atoms with coordination eight (with zero, two and four silver neighbors), for which the LVDOS is shown in figure 8(c). At the high-frequency end, the largest shift is found for the case of Cu atoms with two silver neighbors, followed by those with four silver neighbors. The smallest shift in the high-frequency region is found for the Cu atom with zero silver neighbors, bond lengths ranging from 2.40 to 2.80 Å, for two silver neighbors 2.41 to 2.78 Å and for four silver neighbors 2.43 to 2.82 Å. These results diverge from the trend seen above. The effect of local environment on the features obtained at the high-frequency end of the LVDOS thus points to the need for more accurate analysis based on electronic structure calculations. At the low-frequency end, there is more pronounced deviation of the VDOS from the bulk with loss of coordination: the increase of silver atoms enhances the shift towards low frequency.

Finally, we discuss the vibrational dynamics of Cu atoms with coordination six. In figure 8(d), the LVDOS is shown (for the first category of large bond length) with zero, one and two silver neighbors in the environment. At the high-frequency end, the largest shift is found for atoms with zero and one silver neighbor, with the shortest bond lengths being 2.29 Å and 2.31 Å respectively. For Cu atoms with two silver neighbors, the shortest bond length is 2.41 Å, which shows the smallest shift at the high-frequency end. For the low-frequency end, one notices the complexity of the spectra. However, we can still extract a few trends: the order of enhancement is for Cu atoms with zero, one and two silver neighbors with the largest bond length being 2.65 Å, 2.75 Å and 2.73 Å, respectively.

One would intuitively expect that the larger the bond length, the larger would be the frequency softening. This is not however the case here. In figure 8(e), we report the LVDOS of atoms with coordination six (from the category of short bond lengths) containing zero, one and two silver neighbors. We note that a shift in high frequencies is found only for copper atoms with two silver neighbors (table 1). It is interesting to note that even for the atoms with zero and one silver neighbors with relatively short bond lengths (2.44 Å and 2.39 Å, respectively) the corresponding LVDOS does not show any new features at high frequencies. At the low-frequency end, we note the same trend as shown in figure 8(d), for which increasing the number of silver neighbors combined with the highest bond length, for example, for two silver (2.73 Å), one silver (2.64 Å) and zero silver neighbors (2.52 Å) does not enhance the low-frequency modes. In summary, in addition to the obtained useful trends, the above analysis also points to the fact that complex correlations between coordination and environment introduce some features in the local vibrational densities of states that cannot be adequately accounted for solely on the basis of local environment and bond-length arguments. Further work is needed to address these issues.

3.2.2. Local vibrational density of states of silver atoms in selected nanoparticles. In figures 9(a)–(c), we present the LVDOS of silver atoms with coordination nine, eight and

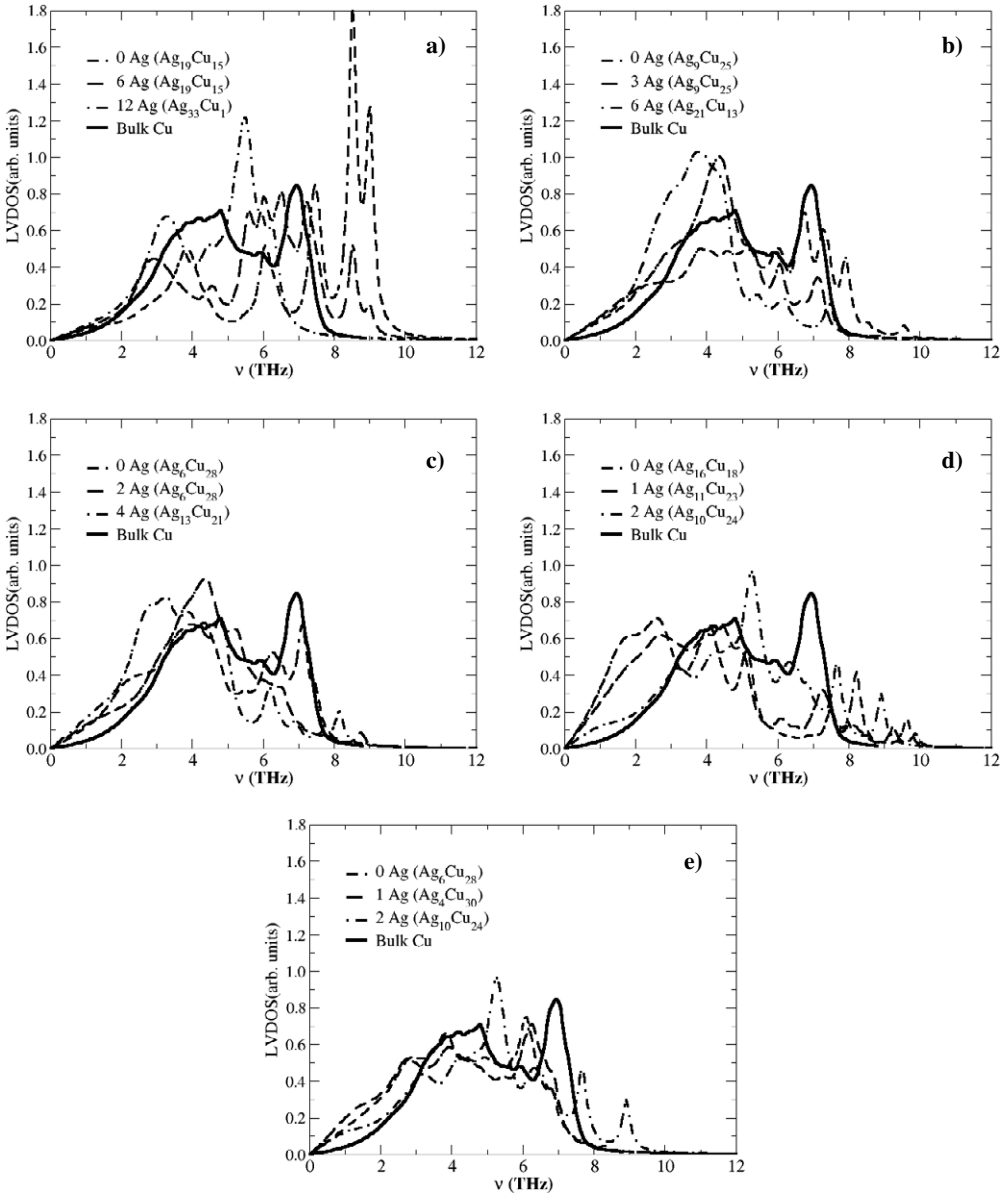

Figure 8. Local vibrational densities of states (LVDOS) of selected copper atoms with coordination (**a**) 12, (**b**) 9, (**c**) 8, (**d**) 6 (large bond length) and (**e**) 6 (short bond length) and elemental environment.

six, following the same procedure as used for copper. Here again the choice of the nanoparticle for the atom in question is reported in the figures. For example, for coordination nine, the Ag atom with zero copper neighbors is chosen from Ag_{34}, while those with three and five copper neighbors are from $Ag_{23}Cu_{11}$. From figure 9(a), we see a shift in the density of states towards high frequencies above the bulk Cu band for the Ag atoms with three and five copper neighbors, the higher shift being for the latter, which can be explained by the bond-length analysis given above. The enhancement at the low-frequency end simply reflects the reduction in the coordination. From figure 9(b), we conclude that the features at high and low frequencies for the atoms with coordination eight are quite similar to those with coordination nine.

The most striking features at both high- and low-frequency ends of the spectrum are associated with silver atoms with coordination six. As for coordinations nine and eight, the high-frequency end contains new modes that are well resolved and arise from environments in which copper is present (figure 9(c)). The lowest bond lengths are 2.47 Å, 2.5 Å and 2.77 Å, for six, three and zero copper neighbors, respectively. Note that the fact that the bond length associated with zero copper neighbors is distinct and larger than that associated with three and six copper neighbors explains the presence of high-frequency modes for the last two cases. It is at the low-frequency end that we notice a large enhancement for all three cases that is much more pronounced than that for the coordinations nine and eight. From the same arguments as used for coordinations nine and eight, however, one would expect to find enhancement for atoms with the highest number of silver neighbors. We note that this is not the case: instead, the highest enhancement of the density of states at the low-frequency end

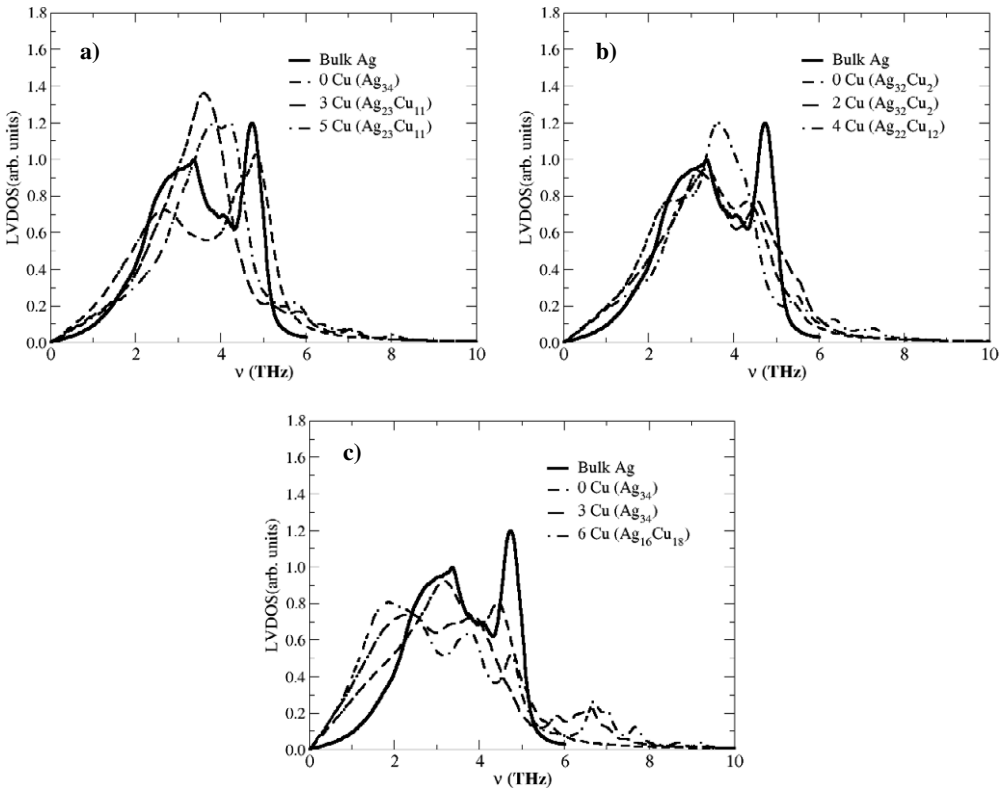

Figure 9. Local vibrational densities of states (LVDOS) of selected silver atoms with coordination (**a**) nine, (**b**) eight and (**c**) six and elemental environment.

of the spectrum is associated with a silver atom with six copper neighbors.

3.3. Vibrational contributions to the excess free energy

The stability of a system and its phase transitions may be explored by studying its thermodynamical properties, in which the vibrational dynamics of a system may play a substantial role. For instance, the role of vibrational free energy in determining the equilibrium structures of bulk-alloy systems has been explored and found to be important [22]. A more recent study of stepped metal surfaces of Cu and Ag showed the vibrational contributions to be a substantial fraction of the step free energy [20]. An equally important and sometimes dominant contribution may arise from configurational entropy. If we were to be comparing the relative stability of a set of isomers for each nanoparticle of a given composition, we would need to include a discussion of the role of configurational entropy. In this work, however, we are restricting ourselves to the specific nanoparticle configurations that Rapallo *et al* [8] have already established as the candidates with the lowest energy for a given set of isomers. We will thus focus only on the assessment of vibrational entropy of a nanoparticle of a fixed configuration.

Our task here is to consider whether the above trend in the contribution of the local vibrational thermodynamic properties to the excess free energy also applies to nanoparticles with only 34 atoms and whether alloying brings some additional characteristics. For this purpose, we have calculated the contribution to the vibrational free energy from each nanoparticle (table 2) and find that it increases monotonically with the number of copper atoms in the nanoparticle. Since contributions to the low-frequency end of the spectrum of VDOS determine vibrational free energy at (relatively) low temperatures, we calculated the percentage contribution of this low-frequency end to the whole spectrum. To do this, we have used the Debye frequencies of bulk copper and silver (6.56 and 4.48 THz, respectively) as the cut-off for the low-frequency 'part' of the LVDOS. We have summarized the percentage contributions in table 2. It is seen clearly from the table that increasing the number of copper atoms (alloying) depletes the low-frequency end of the spectrum, enhancing the contribution of the vibrational dynamics to the free energy. Note that using the Debye frequency of bulk copper instead of silver gives the same trend with higher contributions.

In reference [20], it is shown that the lower the coordination of the atom (on stepped Cu and Ag surfaces), the higher its contribution to the excess free energy. It is also reported that the atom below the step (BNN) has lower contribution than that of the atoms in the bulk (one would expect bulk atoms to have the lowest contribution), and this is attributed to the over-coordination induced by strong structural relaxations. In order to determine how coordination affects the excess free energy, we focus on copper atoms in the Cu_{34} nanoparticle (zero silver neighbors). For the coordinations studied here (12, 9, 8 and 6) we find the corresponding local excess vibrational free energy to be respectively $+12$, -6, -6 and -15 meV/atom. The trend in the contribution of

Table 2. Total vibrational free energies of the nanoparticles and percentage contribution from the low-frequency end of the spectrum for some of the nanoparticles (using the Debye frequency of bulk silver).

Nanoparticle	$F_{\text{vib}}^{\text{total}}$ (eV) (% contribution from low frequency)
Ag_{34}	−1.8226
$Ag_{33}Cu_1$	−1.7802
$Ag_{32}Cu_2$	−1.7529
$Ag_{31}Cu_3$	−1.7345 (73.4%)
$Ag_{30}Cu_4$	−1.7378
$Ag_{29}Cu_5$	−1.6758
$Ag_{28}Cu_6$	−1.6167
$Ag_{27}Cu_7$	−1.6129 (71.4%)
$Ag_{26}Cu_8$	−1.5906
$Ag_{25}Cu_9$	−1.5698
$Ag_{24}Cu_{10}$	−1.5492
$Ag_{23}Cu_{11}$	−1.5295
$Ag_{22}Cu_{12}$	−1.5117
$Ag_{21}Cu_{13}$	−1.4903
$Ag_{20}Cu_{14}$	−1.4673
$Ag_{19}Cu_{15}$	−1.4289
$Ag_{18}Cu_{16}$	−1.4361
$Ag_{17}Cu_{17}$	−1.4351 (65.3%)
$Ag_{16}Cu_{18}$	−1.4139
$Ag_{15}Cu_{19}$	−1.3773
$Ag_{14}Cu_{20}$	−1.3600
$Ag_{13}Cu_{21}$	−1.3457
$Ag_{12}Cu_{22}$	−1.3169
$Ag_{11}Cu_{23}$	−1.3060
$Ag_{10}Cu_{24}$	−1.1530 (53.4%)
Ag_9Cu_{25}	−1.2652
Ag_8Cu_{26}	−1.1452
Ag_7Cu_{27}	−1.0826 (51.2%)
Ag_6Cu_{28}	−1.1363
Ag_5Cu_{29}	−1.1018
Ag_4Cu_{30}	−1.0599
Ag_3Cu_{31}	−1.0322 (48.6%)
Ag_2Cu_{32}	−0.9830
Ag_1Cu_{33}	−0.9812
Cu_{34}	−0.9795

the under-coordinated atoms is thus in accord with what has been reported earlier [20]. The most interesting contribution comes from coordination 12, whose opposite sign reflects the effect of over-coordination, again in agreement with the earlier study on extended systems, except that here the contribution is much larger. For nanoparticles, the over-coordination of the inner atoms results from the global shrinking that the finite size systems experience [19]. For the case of silver atoms with coordinations nine, eight and six, we turn to the contribution of the atoms in the Ag_{34} nanoparticle (zero copper neighbors). We find the contribution to be 0, −4 and −7 meV/atom for coordinations nine, eight and six, respectively. The trend observed here is qualitatively similar to that found for the metal surfaces [21]. We summarize our results for the vibrational entropic contribution for the full set of 35 nanoparticles in figure 10, which shows that the inclusion of the vibrational contribution to the free energy does not introduce noticeable changes in the relative quantities for these nanoparticles. Clearly, the complexity in the local environments leads to both positive and negative contributions to vibrational entropy, making the total contribution small relative to that of the structural energy of the nanoparticle.

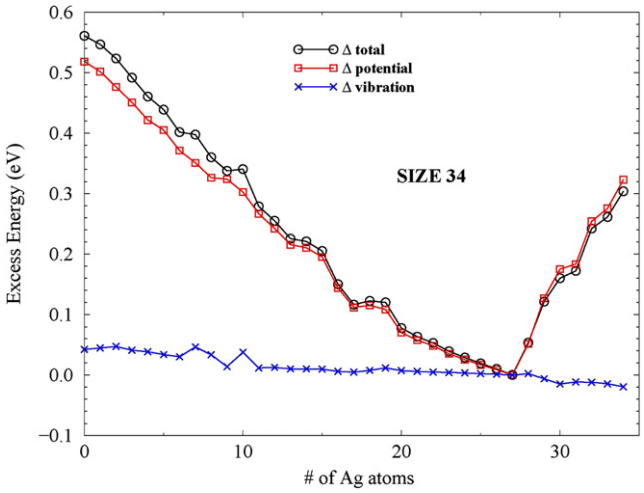

Figure 10. The potential, vibrational and total excess energy of the nanoparticles.

3.4. Mean square vibrational amplitudes and Debye temperature

In an earlier study on vicinal metal surfaces [21], it was found that the mean square vibrational amplitude is enhanced for low-coordination atoms and the Debye temperature is reduced to about two-thirds of the bulk value. In this section we examine the mean square vibrational amplitudes and the Debye temperature of selected atoms in the nanoalloy to see if the effect is similar to that on vicinal surfaces.

The local mean square vibrational amplitudes calculated within the harmonic approximation for copper (silver) atoms with coordination 12, 9, 8 and 6 (9, 8 and 6) are presented in figure 11 (12). As an example, we discuss deviations from the bulk value at 300 K. Starting with copper atoms, for coordination 12 (figure 11(a)) the largest deviation (0.005 $Å^2$) from the bulk value (0.0325 $Å^2$) is found for the case which has the highest number of silver nearest neighbors. For coordinations nine and eight, we find that the higher the number of silver neighbors, the more the mean square vibrational amplitudes deviate from the bulk (0.022 $Å^2$ and 0.04 $Å^2$, respectively). However, for Cu atoms with coordination six (in the large-bond-length regime) the trend is the opposite and more striking: an increase in the number of silver neighbors results in a decrease in the mean square vibrational amplitudes. This latter trend can be traced back to the low-frequency part of the VDOS for such atoms (figure 8(d)), which resembles the bulk VDOS. The largest deviation is found to be 0.15 $Å^2$ (30 times larger than that of coordination 12). For the short-bond-length case, the same trend is reported in figure 11(e), with a deviation of 0.1 $Å^2$ (for zero silver neighbors).

Turning to the case of silver atoms with coordination nine, we note from figure 12(a) that a decrease in the number of copper neighbors brings an increase in the mean square vibrational amplitude, with a deviation from that of the bulk of about 0.04 $Å^2$. When the coordination is reduced to eight (figure 12(b)), regardless of the number of copper

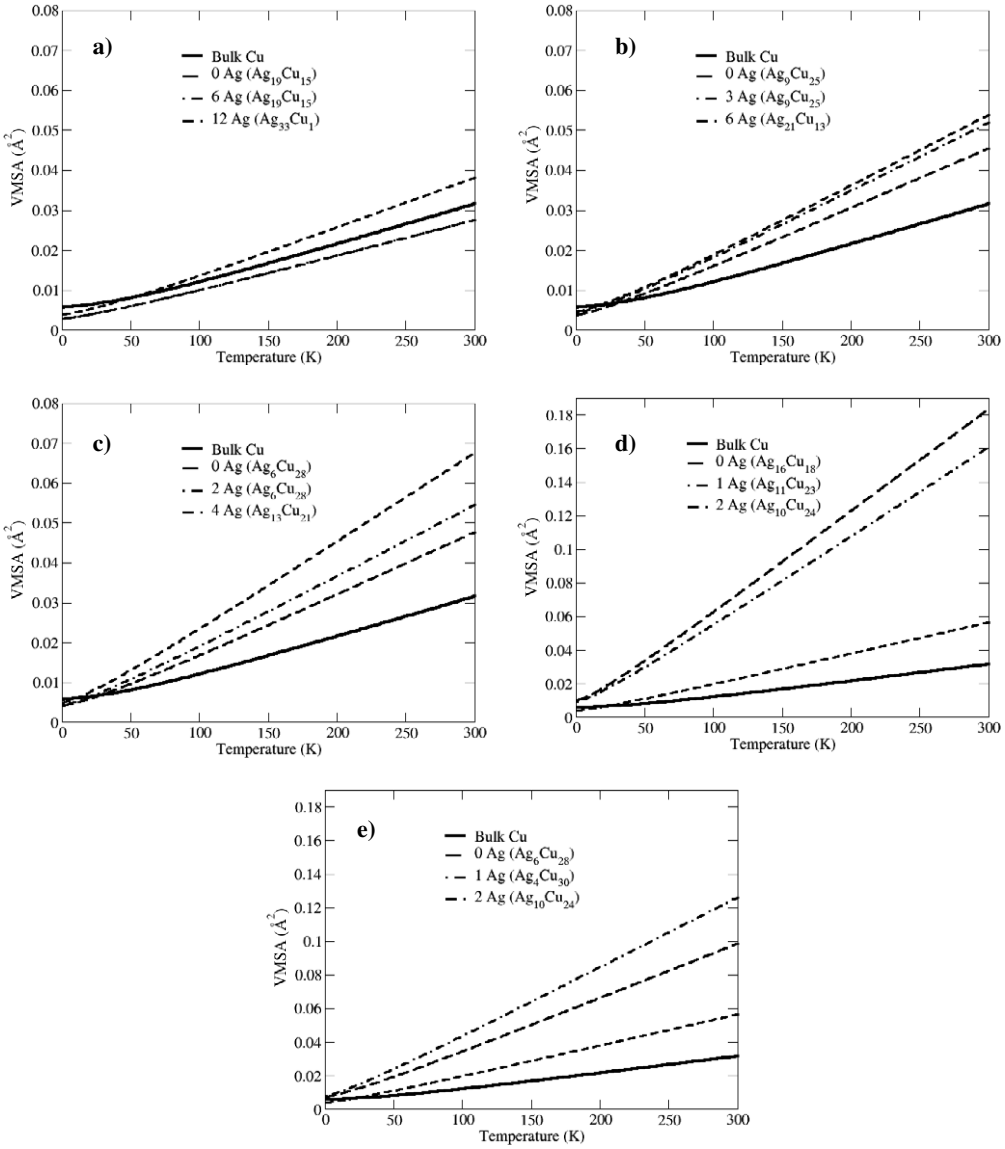

Figure 11. Mean square vibrational amplitudes of copper atoms with coordination (**a**) 12, (**b**) 9, (**c**) 8, (**d**) 6 (large bond length) and (**e**) 6 (short bond length) and elemental environment.

neighbors, the mean square amplitudes become almost the same (∼0.075 Å^2) and the deviation is found to be the same as that for atoms with coordination nine (0.04 Å^2). We thus conclude that local coordination has less effect on the mean square vibrational amplitude of silver than it does on that of copper atoms, as already reported [20]. For silver atoms with coordination six (figure 12(c)), as in the case of copper atoms for the same coordination, we see that addition of more copper atoms induces larger mean square vibrational amplitudes, with a deviation of 0.1 Å^2 from the bulk value.

Note that mean square vibrational amplitude, being a local quantity, changes dramatically from one atom to another in the nanoparticle. Experiments, on the other hand, would be more amenable to the measurements of a global quantity, reflecting an averaged value, such as the Debye temperature, which is related to the mean square vibrational amplitude as expressed in equation (6). We have calculated the Debye temperature of each nanoparticle studied here using the mean square vibrational amplitudes of all the atoms for the nanoparticle. This *average* Debye temperature is reported in table 3 along with a breakdown into contributions from copper and silver atoms. The upper and lower limits of the average Debye temperature are found to be 69 and 88 K, respectively. For copper (silver) atoms, the average Debye temperatures are found to be in the range of 86–111 K (60–71 K), which is about one-third of the Debye temperature of the corresponding bulk. From table 3, it is clear that the average Debye temperature of the nanoparticles does increase with the increase of copper atoms. The increase is, however, not linear.

To examine the critical role of the atomic coordination in controlling local dynamics, we have calculated the Debye temperatures for copper and silver atoms with coordinations ranging from 6 to 12. We present here only the Debye temperatures of atoms from Cu_{34} and Ag_{34} nanoparticles for which we find copper atoms with coordination 12, 9, 8 and

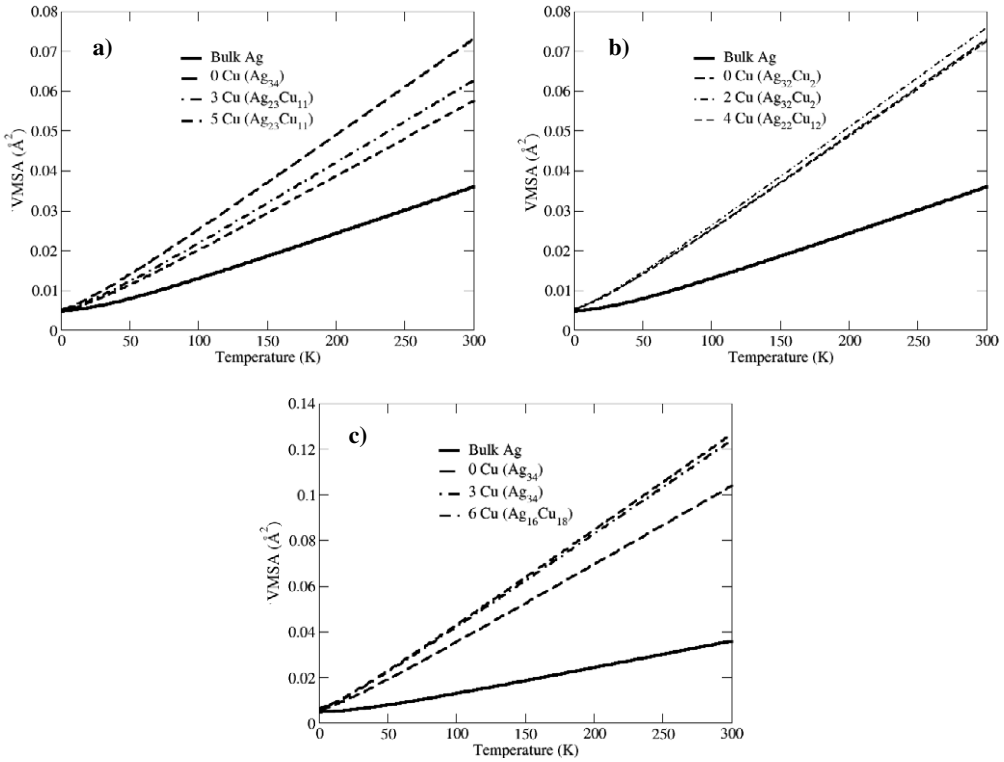

Figure 12. Mean square vibrational amplitudes of silver atoms with coordination (**a**) nine, (**b**) eight and (**c**) six and elemental environment.

6 to have a Debye temperature 103, 83, 81–96, 73–87 K, respectively. The Debye temperatures for coordinations eight and six have upper and lower limits that reflect the variations in bonding for these specific coordinations, as has already been discussed. If we consider the lower limit in the temperature range, we note the same correlations as predicted for the vicinal surfaces [21]. For silver atoms in the nanoparticle, we find the Debye temperature to be 87, 75, 72 and 62 K for coordinations 12, 9, 8 and 6, respectively. The correlation between the Debye temperature and coordination found for copper is also observed for silver atoms.

From table 3, it is worth noting that there is a sharp change in the average Debye temperature for $Ag_{29}Cu_5$ and $Ag_{28}Cu_6$ nanoparticles. On examining the individual contributions to the Debye temperature from the copper and silver atoms, we find that the contribution from the former ranges from 104.5 to 110.4 K for $Ag_{28}Cu_6$ and from 84.5 to 100.2 K for $Ag_{29}Cu_5$. The average contributions from the copper atoms then become 107.9 and 89.9 K for the $Ag_{28}Cu_6$ and $Ag_{29}Cu_5$ nanoparticles, respectively (see table 3). For the same nanoparticles, the average Debye temperatures of the silver atoms are found to be 71.0 K and 68.9 K, nearly the same as for $Ag_{28}Cu_6$ and $Ag_{29}Cu_5$ nanoparticles, respectively. The calculated dip in the average Debye temperature thus arises mainly from the individual contributions of the copper atoms of these nanoparticles. The structural motifs of these two particles are different from each other, and neither is symmetric. Interestingly, while copper atoms in the $Ag_{28}Cu_6$ nanoparticle have coordination 12, for those in $Ag_{29}Cu_5$ the coordination varies from 10 to 12.

4. Conclusions

A detailed study of the family of Ag_nCu_{34-n} nanoparticles shows interesting trends 'upon alloying' in bond-length variations, vibrational dynamics and thermodynamics. Through arguments based on local coordination and elemental environment these characteristics can be systematically rationalized. In particular, we find the average bond length for copper atoms to depend strongly on both coordination and elemental environment. It increases monotonically by 0.25 Å as the number of Ag nearest neighbors varies from 0 to 12. However, these variations in the average bond length are less pronounced for silver atoms. For the copper atoms with low coordination (6 and 8), a global analysis of the bond length reveals two regions (with short and long average bond length). This bi-modal behavior, which goes beyond coordination and direct environment, is the subject of a second degree environmental analysis (second neighbors) and will be reported elsewhere along with a detailed study using density functional theory [16].

We find that increasing the ratio of copper to silver atoms (alloying) induces systematic stiffening in the force field, inducing a shift towards high frequencies in the vibrational density of states. On the other hand, the low-frequency end of the spectrum is found to be similar to that of single-element nanoparticles, which shows a linear dependence on the frequency.

We find that the (total) vibrational free energy of the family of Ag_nCu_{34-n} nanoparticles increases monotonically with the number of copper atoms in the system. The effect of coordination on the excess vibrational free energy shows qualitative similarities to the atoms on vicinal surfaces and in

Table 3. The average Debye temperature $\langle\theta_D\rangle$ of the nanoparticles, together with those from constituent Ag and Cu atoms.

Nanoparticle	$\langle\theta_D\rangle$ of nanoparticles (K)	$\langle\theta_D\rangle$ of Cu atoms (K)	$\langle\theta_D\rangle$ of Ag atoms (K)
Ag_{34}	69.6	—	69.6
$Ag_{33}Cu_1$	70.9	104.7	69.8
$Ag_{32}Cu_2$	71.6	99.8	69.8
$Ag_{31}Cu_3$	71.5	98.1	68.9
$Ag_{30}Cu_4$	69.2	85.6	67.0
$Ag_{29}Cu_5$	71.9	89.9	68.9
$Ag_{28}Cu_6$	77.5	107.9	71.0
$Ag_{27}Cu_7$	78.3	110.9	69.9
$Ag_{26}Cu_8$	78.7	109.2	69.3
$Ag_{25}Cu_9$	79.2	107.9	68.9
$Ag_{24}Cu_{10}$	79.7	107.0	68.4
$Ag_{23}Cu_{11}$	80.3	106.3	67.8
$Ag_{22}Cu_{12}$	80.5	105.0	67.1
$Ag_{21}Cu_{13}$	80.9	104.4	66.4
$Ag_{20}Cu_{14}$	81.3	103.4	65.8
$Ag_{19}Cu_{15}$	82.4	102.9	66.3
$Ag_{18}Cu_{16}$	82.3	101.9	64.8
$Ag_{17}Cu_{17}$	82.2	102.5	61.8
$Ag_{16}Cu_{18}$	82.9	100.9	62.7
$Ag_{15}Cu_{19}$	83.1	98.2	63.9
$Ag_{14}Cu_{20}$	83.4	97.6	63.1
$Ag_{13}Cu_{21}$	83.6	97.6	61.0
$Ag_{12}Cu_{22}$	84.5	97.2	61.1
$Ag_{11}Cu_{23}$	84.5	95.7	60.9
$Ag_{10}Cu_{24}$	85.6	93.9	65.8
Ag_9Cu_{25}	85.2	94.3	59.9
Ag_8Cu_{26}	87.5	95.1	62.6
Ag_7Cu_{27}	86.1	95.7	64.1
Ag_6Cu_{28}	84.9	88.3	69.5
Ag_5Cu_{29}	84.9	88.1	66.2
Ag_4Cu_{30}	87.2	89.7	68.5
Ag_3Cu_{31}	87.2	89.0	68.4
Ag_2Cu_{32}	88.1	89.3	67.5
Ag_1Cu_{33}	86.6	87.1	69.8
Cu_{34}	87.4	87.4	—

single-element nanoparticles, though substantial quantitative differences appear. The local vibrational mean square amplitudes present strong correlations with coordination. We also find that the calculated average Debye temperatures of these nanoparticles increase with the number of copper atoms, but this change is not linear. Also, the Debye temperature of copper (silver) atoms in the nanoparticles is found to be about one-third of the bulk as compared to a ratio of two-thirds of the bulk reported for the atoms on stepped surfaces of Ag and Cu.

Acknowledgments

We thank Riccardo Ferrando for providing us with the initial configuration of the nanoalloys and Sophie Exdell for help in visualizing and analyzing the data set. We are grateful to Lyman Baker for critical reading of the manuscript. TSR appreciates fruitful discussions with Miguel Kiwi. This work was supported in part by DOE under grant DE-FG02-07ER46354.

References

[1] Jortner J 1992 *Z. Phys.* D **24** 247
Johnston R L 1998 *Phil. Trans. R. Soc.* A **356** 211
[2] Jensen P 1999 *Rev. Mod. Phys.* **71** 1695
Ashman C, Khanna S N, Liu F, Jena P, Kaplan T and Mostoller M 1997 *Phys. Rev.* B **55** 15868
[3] Molenbroek A M, Haukka S and Clausen B S 1998 *J. Phys. Chem.* B **102** 10680
Kreibig U and Vollmer M 1995 *Optical Properties of Metal Clusters* (Berlin: Springer)
Cottancin E, Lerme J, Gaudry M, Pellarin M, Vialle J L, Broyer M, Prevel B, Treilleux M and Melinon P 2000 *Phys. Rev.* B **62** 5179
Portales H, Saviot L, Duval E, Gaudry M, Cottancin E, Pellarin M, Lerme J and Broyer M 2002 *Phys. Rev.* B **65** 165422
Giorgio S and Henry C R 2002 *Eur. Phys. J. Appl. Phys.* **20** 23
Moskovits M, Srnova Sloufova I and Vlckova B 2002 *J. Chem. Phys.* **116** 10435
Tada H, Suzuki F, Ito S, Akita T, Tanaka K, Kawahara T and Kobayashi H 2002 *J. Phys. Chem.* B **106** 8714
Valden M, Lai X and Goodman D W 1998 *Science* **281** 1647
Molina L M and Hammer B 2003 *Phys. Rev. Lett.* **90** 206102
Haruta M 1997 *Catal. Today* **36** 153
Lee S, Fan C, Wu T and Anderson S L 2005 *J. Chem. Phys.* **123** 124710
[4] Rossi G, Rapallo A, Mottet C, Fortunelli A, Baletto F and Ferrando R 2004 *Phys. Rev. Lett.* **93** 105503
[5] Pearson W B 1972 *The Crystal Chemistry and Physics of Metals and Alloys* (New York: Wiley)
[6] Rosato V, Guillopé M and Legrand B 1989 *Phil. Mag.* A **59** 321
Guillopé M and Legrand B 1989 *Surf. Sci.* **215** 577
Cleri F and Rosato V 1993 *Phys. Rev.* B **48** 22
[7] Baletto F, Mottet C and Ferrando R 2002 *Phys. Rev.* B **66** 155420
Baletto F, Mottet C and Ferrando R 2003 *Phys. Rev. Lett.* **90** 135504
Baletto F, Mottet C, Rossi G, Rapallo A and Ferrando R 2004 *Surf. Sci.* **566** 192
Rossi G, Rapallo A, Mottet C, Fortunelli A, Baletto F and Ferrando R 2004 *Phys. Rev. Lett.* **93** 105503
[8] Rapallo A, Rossi G, Ferrando R, Fortunelli A, Curley B C, Lloyd L D, Tarbuck G M and Johnston R L 2005 *J. Chem. Phys.* **122** 194308
[9] Ferrando R, Jellinek J and Johnston R L 2008 *Chem. Rev.* **108** 845
[10] Darby S, Mortimer-Jones T V, Johnston R L and Roberts C 2002 *J. Chem. Phys.* **116** 1536
[11] Asta M and Ozoliņš V 2001 *Phys. Rev.* B **64** 094104
Anthony L, Okamoto J K and Fultz B 1993 *Phys. Rev. Lett.* **70** 1128
Fultz B, Anthony L, Nagel L J, Nicklow R M and Spooner S 1995 *Phys. Rev.* B **52** 3315
Nagel L J, Anthony L and Fultz B 1995 *Phil. Mag. Lett.* **72** 421
Anthony L, Nagel L J, Okamoto J K and Fultz B 1994 *Phys. Rev. Lett.* **73** 3034
[12] Press W, Teukolsky S, Vetterling W and Flannery B 1992 *Numerical Recipes in Fortran* (Cambridge: Cambridge University Press)
[13] Daw M S, Foiles S M and Baskes M I 1993 *Mater. Sci. Rep.* **9** 251
[14] Foiles S M, Baskes M I and Daw M S 1986 *Phys. Rev.* B **33** 7983
Daw M S, Foiles S M and Baskes M I 1983 *Mater. Sci. Rep.* **9** 251
[15] Durukanoglu S, Kara A and Rahman T S 2003 *Phys. Rev.* B **67** 23405

[16] Yildirim H, Kara A and Rahman T S, unpublished
[17] Ortigoza M A and Rahman T S 2008 *Phys. Rev.* B **77** 195404
[18] Mottet C, Rossi G, Baletto F and Ferrando R 2005 *Phys. Rev. Lett.* **95** 035501
[19] Kara A and Rahman T S 1998 *Phys. Rev. Lett.* **81** 1453
[20] Durukanoglu S, Kara A and Rahman T S 2003 *Phys. Rev.* B **67** 235405
[21] Kara A and Rahman T S 2005 *Surf. Sci. Rep.* **56** 159–87
[22] Anthony L, Okamoto J K and Fultz B 1993 *Phys. Rev. Lett.* **70** 1128
Nagel L J, Anthony L and Fultz B 1995 *Phil. Mag. Lett.* **72** 421
Bogdanoff P D, Fultz B and Rosenkranz S 1999 *Phys. Rev.* B **60** 3976